Behavioral Ecology and Sociobiology (2023) 77:63
https://doi.org/10.1007/s00265-023-03332-8

ORIGINAL ARTICLE

Flight behaviours and energy savings in adult and juvenile house martins (*Delichon urbicum*) foraging near their breeding colony

Geoffrey Ruaux[1] · Kyra Monmasson[1] · Tyson L. Hedrick[2] · Sophie Lumineau[1] · Emmanuel de Margerie[1]

Received: 28 September 2022 / Revised: 3 May 2023 / Accepted: 5 May 2023 / Published online: 27 May 2023

Abstract

Foraging is an extremely important behaviour for birds, especially during the breeding season, when they have to carry the cost of incubation and chick rearing, in addition to their own energy needs. Aerial insectivores perform most of their foraging behaviours in flight, so they have evolved various adaptations to reduce energy output whilst increasing energy input during this critical period. In this study, we recorded the 3D flight behaviours of 100 house martins (*Delichon urbicum*) flying near their colony during the breeding season in Rennes, France. We give a first description of the distribution of several kinematic and biomechanical variables (horizontal and vertical speed, rates of change in kinetic and potential energy, turning radius of curvature and centripetal force), compare flapping and gliding flight, and describe several strategies used by flying house martins to save energy, such as environmental energy extraction (thermal soaring) and optimisation of flight speed according to wind speed and direction. We also report an effect of temperature, solar radiation and humidity on the mean vertical speed of gliding birds, highlighting the effect of weather on the availability of external energy sources such as thermal updrafts. Finally, we compare the distribution of flight speed and vertical speed between 5 juveniles identified using magnified photographs and 20 adults recorded during the same field sessions, and we show that during flapping flight, juveniles exhibit higher, more variable airspeed than adults, suggesting that their flight behaviours are not immediately fine-tuned after leaving the nest.

Significance statement

Aerial insectivores use various strategies to reduce the cost of foraging flight. Using an optical tracking method, we recorded the 3D flight behaviours of house martins (*Delichon urbicum*) flying near their colony during the breeding season. We describe the distribution of several biomechanical variables and show that house martins use external energy sources such as thermal updrafts and also adapt their airspeed to wind speed and direction, supporting the predictions on optimal cost of transport in birds. Moreover, juveniles were also recorded, and they show a greater variability in flight speed, possibly because they may not be as accurate as adults in finely adjusting their speed and altitude. Our findings add to the existing literature showing energy-saving strategies in aerial insectivores, and also study an ontogenetical aspect rarely explored.

Keywords Energy · Wind · Kinematics · Ontogeny

Introduction

Foraging is a behaviour of crucial importance in the life cycle of birds, especially during the breeding season. During incubation, parents have to cope with various constraints and invest time and energy (Shaffer et al. 2003). When chicks hatch, parents still have to dedicate some time to warm or protect them in many species, and they additionally have to cover the food needs of an entire brood (Ydenberg 1994; Markman et al. 2002).

Communicated by B. Voelkl

✉ Emmanuel de Margerie
emmanuel.demargerie@univ-rennes1.fr

[1] Univ Rennes, Normandie Univ, CNRS, EthoS (Éthologie Animale Et Humaine) - UMR 6552, 35000 Rennes, France

[2] University of North Carolina at Chapel Hill, Chapel Hill, NC 27599, USA

Aerial insectivores, like swifts, swallows and martins, have to fly continuously and to perform flight manoeuvres while foraging (Bryant and Turner 1982; Kacelnik and Houston 1984). Swifts, swallows and martins feed their chicks with a food bolus constituted of tens to hundreds of arthropods (Bryant and Turner 1982; Gory 2008), which avoids having to fly back and forth between the nest and the foraging patches for each individual prey. During foraging, maximisation of energy intake per unit time is obviously important, but energy consumed during flight is considerable, and the foraging strategy must be a balance between the energy output during flight and the energy intake from feeding (Rayner 1982). Thus, flying at a low cost is of paramount importance for foraging aerial insectivores.

Various behavioural adaptations exist to reduce flight energy expenditures. For example, some aerial insectivores are able to extract energy from their environment during foraging. Common swifts (*Apus apus*) can glide in thermal updrafts and use wind gusts and wind gradients to save energy (de Margerie et al. 2018; Hedrick et al. 2018), while barn swallows (*Hirundo rustica*) also use wind gradients to gain potential and kinetic energy during turns (Warrick et al. 2016).

Additionally, wind speed and direction may also influence the flight behaviours of foraging aerial insectivores. Indeed, theory predicts that birds should adjust their airspeed when flying upwind or downwind for energetically optimal cost of transport in the ground reference frame (Pennycuick 1978). The maximum range speed of birds (the airspeed at which the distance travelled for a given amount of energy consumed is maximised) is influenced by wind, and birds optimising their energy expenditure per unit of distance should increase their airspeed when flying upwind and decrease it when flying downwind. This phenomenon has been confirmed in migrating or commuting birds (Wakeling and Hodgson 1992; Hedenström et al. 2002; Kogure et al. 2016; Sinelschikova et al. 2019) and also in the common swift while foraging on aerial insect prey (Hedrick et al. 2018), probably because of the presence of its nest at a fixed ground position.

In addition to wind, other weather variables might have an effect on the flight behaviours of aerial insectivores, such as temperature, solar radiation or humidity, because they influence the availability and movement patterns of aerial insect prey (Lack and Owen 1955; Bryant 1973; Wainwright et al. 2017), and also the availability of external energy sources such as thermal updrafts (Poessel et al. 2018).

Finally, very little is known about the ontogeny of foraging and energy-saving flight behaviours within an individual. Since foraging flight is a complex behaviour, it is possible to hypothesise that juvenile birds may not be as efficient as adults in all aspects immediately after fledging, as is the case in many species for various flight behaviours (see review in Ruaux et al. 2020).

The house martin (*Delichon urbicum*) is a socially monogamous, coursing insectivore nesting in colonies, in which both sexes incubate and feed the chicks (Bryant 1979; Whittingham and Lifjeld 1995; del Hoyo et al. 2020). They lay up to three clutches per year, and each clutch is composed of one to seven (most often four to five) eggs (del Hoyo et al. 2020). Bryant and Westerterp (1980) studied the energy budget of breeding house martins and calculated that each parent spent around 6 h per day away from the nest during incubation, and that a bird foraging at the highest observed rate in optimal conditions during this time would gather energy only 6% in excess of its requirements, leaving little margin for other activities and lower foraging rates in poorer conditions. When feeding chicks, parents spend more time in flight but have to meet the energy needs of their brood in addition to their own needs. Thus, breeding house martins should spend most of their time actively foraging and should mostly be travelling or searching for food otherwise. In this context, studying the flight behaviours of house martins near a colony during the breeding period may improve understanding of the characteristics of flight during this crucial period, and identify possible means by which these birds reduce their energy expenditures.

In the present study, we measured the 3D flight trajectories of house martins using rotational stereo-videography (RSV; de Margerie et al. 2015) to describe biomechanical characteristics of their flight. One of our goals was to give a first description of the "flight envelope" of house martins in a field study to understand how they use the aerial habitat near their colony during the breeding period. We also tested some of the hypotheses related to energy savings in aerial insectivores: we studied the gliding and flapping behaviours of house martins to determine if they use external energy sources such as thermal currents, wind gusts and wind gradients, and if weather conditions could influence these behaviours. Then, we tested if house martins change their airspeed depending on wind direction to optimise their energy expenditure in the ground reference frame. Finally, we investigated if juvenile house martins differ from adults in some aspects of their flight behaviours.

Materials and methods

All symbols and abbreviations used in our analyses can be found in Table 1.

Recording site and time

House martins were recorded near a colony located in Rennes, France (Fig. 1; see also Fig. S1 for a ground view

Table 1 List of symbols and abbreviations

a	Bird acceleration vector in the ground reference frame
a_Z	Bird vertical acceleration
A	Wind speed vector
F	Mass-specific centripetal force
g	Magnitude of gravitational acceleration
P	Mass-specific kinematic power (sum of rates of change in mass-specific kinetic and potential energy)
P_k	Mass-specific rate of change in kinetic energy
P_p	Mass-specific rate of change in potential energy
R	Instantaneous radius of curvature
RSV	Rotational stereo-videography
s_a	Bird speed in the air reference frame
s_{ha}	Bird horizontal speed in the air reference frame
s_w	Wind speed
s_Z	Bird vertical speed
v	Bird velocity vector in the ground reference frame
$\mathbf{v}_a$	Bird velocity vector in the air reference frame
X, Y, Z	Bird Cartesian coordinates in the ground reference frame
Θ	Azimuthal angle measurement from RSV
P	Radial distance measurement from RSV
Φ	Elevation angle measurement from RSV
·	Dot-over character, indicating first derivative with respect to time
··	Double dot-over character, indicating second derivative with respect to time
Subscript 1s	Variable averaged over 1 s (10 consecutive frames where flight behaviour did not change)

of the experimental setup). The breeding house martins are present in the colony from May to September, and the colony is composed of several tens of nests built on buildings (3- to 6-floor), surrounded by an urban landscape, with mainly roads, a wide lawn and urban gardens. The RSV device was located on a small hill to the northwest of the colony (48°07′45.55″N 1°40′42.88″W), with a panoramic view over the wide lawn and urban gardens above which the house martins were often flying.

Nine recording sessions took place from May to July 2021, corresponding to the time when house martins are raising their first brood in this region of France (del Hoyo et al. 2020). Recordings took place in the morning between 9:30 and 12:00 h, when house martins were regularly observed flying near the colony.

During each field session, a GILL Instruments MaxiMet GMX501 weather station (Lymington, UK) with ultrasonic anemometer was set up on a tripod to measure the approximate wind speed and direction experienced by house martins flying near the colony. We placed the anemometer at 2 m height above the ground, in the wide lawn located west to the colony to minimise proximity with any tree or building (see Fig. 1). The weather station also recorded temperature, solar radiation, humidity and atmospheric pressure. All variables were recorded at 1 Hz and were averaged over the duration of each trajectory.

Rotational stereo-videography (RSV)

RSV is an optical tracking technique based on a set of mirrors projecting a stereo image of the animal on the sensor of a single camera (de Margerie et al. 2015). The distance to the animal is measured by analysing the lateral shift between animal image pairs. The rigid assembly of the camera and mirrors can rotate horizontally and vertically on a tripod and fluid video head. Whilst the operator rotates the device to keep the moving animal's image within the sensor frame, the aiming angles are recorded by angular encoders. The geometrical combination of distance and aiming angles (corrected for the position of the animal image on the sensor) yields a 3D record of the animal's movement.

We used an updated RSV device (Fig. S2) with a 1-m base length between the lateral mirrors, a Manfrotto 504HD fluid head (Cassola, Italy) equipped with 17-bit digital angular encoders (Kübler Sendix F3673, Villingen-Schwenningen, Germany), recording aiming angles at 200 Hz through an Arduino Mega microcontroller (www.arduino.cc), and an Adafruit Data logging shield (New York, USA). The device

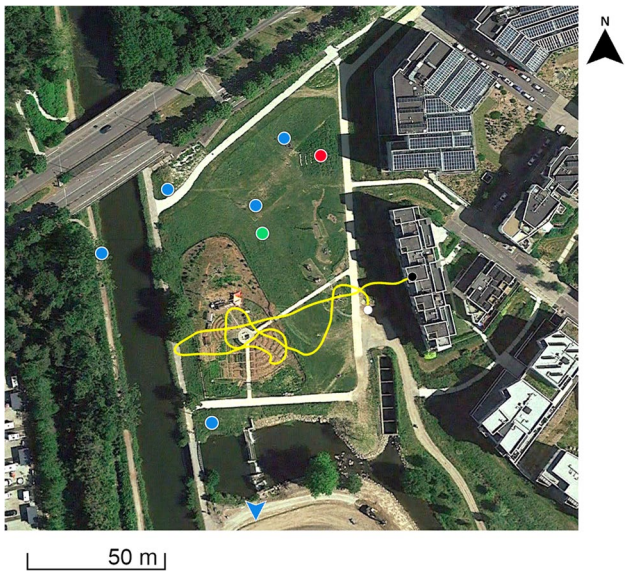

Fig. 1 Aerial view of the recording site. The red dot indicates the location of the RSV device, the green dot indicates the location of the weather station, and blue dots indicate the location of calibration points. The blue arrow indicates the direction of the sixth calibration point, located 410 m away from the RSV device and not represented here for legibility. The yellow line shows an example of a trajectory, with the white dot marking the beginning and the black dot marking the end. The colony is located on all the buildings on the right side of the aerial view (e.g. where the example trajectory ends). Source for aerial view: Google Earth

was equipped with a Panasonic DC-GH5S camera (Osaka, Japan) recording 4096 × 2160-pixel frames at 60 Hz (150 Mbps H.264 compression) from a 19 × 10 mm sensor area. We used a Nikon AF 105 mm f/2 lens (Tokyo, Japan), providing a 5.2° horizontal field of view for each side of the stereo image. To get well exposed and sharp images, we used a 1/1300–1/640-s shutter speed and f/11 aperture, with ISO 1000–2500, depending on available light conditions. To help tracking the fast-flying birds, the camera was equipped with a Nikon DF-M1 dot sight viewfinder (Osaka, Japan).

Calibration and location error

To calibrate the distance measure, which is based on the lateral offset between left and right images of the bird, we recorded six conspicuous targets (signs, street lamps, trees) located at fixed distances from the RSV device, from 16 to 410 m. The real distance to these targets was measured with a Nikon Forestry Pro hand laser rangefinder (Tokyo, Japan).

The random positioning error was approximately 0.04 m at 25 m, 0.10 m at 50 m and 0.34 m at 100 m (Fig. S3).

Recording methods and data classification

During each field session, we recorded any house martins seen flying at 25–100 m from the RSV device (i.e. convenience sampling), and each individual was followed until it was lost by the operator. To minimise pseudoreplication, we made sure to record a different individual at the end of each recording. Despite this precaution, pseudoreplication may be present to some extent in our data since many individuals were flying back and forth between their nest and the nearby gardens. However, we assume pseudoreplication to be modest, since we recorded 100 trajectories near the colony composed of several tens of pairs.

To analyse a sufficient and comparable portion of trajectories, recordings lasting less than 30 s were removed. Retained videos were subsampled from 60 to 10 Hz to ensure that the number of frames was manageable for digitising, yet still appropriate to describe flight behaviours at a fine temporal scale.

Moreover, recordings where the bird was out of frame during more than 10 consecutive frames (i.e. more than 1 s missing at 10 Hz) were also removed (with a 5.2° field of view, the operator occasionally struggled to continuously follow the bird's path with the camera). The resulting sample had 97 trajectories with a homogeneous distribution over the nine field sessions (between 9 and 12 trajectories per session).

During each recording, photographs were taken with a greater magnification using a second camera mounted on the RSV device (Panasonic DMC-GH4 with a Nikon AF 200 mm f/4 lens) to have a clearer view of the plumage of each bird and to be able to identify juveniles, which are recognised mainly by the white tips of their tertials (Blasco-Zumeta and Heinze 2014). Five juveniles could be identified during two field sessions in the first half of July, consistent with the breeding phenology of house martins (del Hoyo et al. 2020). Three of these juveniles had trajectories lasting less than 30 s (15, 23 and 29 s). These juveniles were added to the dataset to ensure a minimal sample size for juveniles, increasing the total to 100 trajectories (95 adults and 5 juveniles), with a median duration of 37.5 s and a total duration of 4512 s.

To study the link between house martins' behaviours and biomechanical variables, the flapping behaviour was labelled on each frame by direct observation of the recorded videos, as either "gliding", "flapping" or "not visible" when the bird was too far or flew in front of a very textured background (foliage). Only birds performing at least one full downstroke and upstroke cycle were categorised as flapping, because they occasionally performed short manoeuvring wing movements during gliding.

It was not possible to record data blind because our study involved focal animals in the field.

Track processing

Stereo videos and angular records were processed with MATLAB r2018b (The MathWorks, Natick, MA, USA). To digitise the bird's locations in each video frame, the pixel at the centroid of the bird's body in the left half of the frame was selected as the left point of interest (POI), either manually or with the help of semi-automatic tracking (DLTdv version 8a; Hedrick 2008). Then, automated normalised cross-correlation between a 31 × 31-pixel area around the left POI and the right half of the image was used to find the corresponding right POI. Automated matching of right POI was sometimes misled by variable backgrounds (sky, foliage, buildings), and thus was visually checked and manually corrected when needed. The bird's distance from the RSV device was then computed based on the calibration reference.

RSV tracking yields spherical coordinates of the bird for each video frame (i.e. azimuth angle, elevation angle and distance from the device; Θ, Φ and P respectively). Raw coordinate series contain noise, due to (i) theoretical positioning uncertainty (increasing with P^2; see de Margerie et al. 2015) and (ii) POI random positioning error in stereo images, which was exacerbated by variable image backgrounds. Consequently, we smoothed the raw spherical coordinate series using quintic splines (which allow non-zero acceleration at the sequence ends), with an error tolerance based on the sum of (i) the per-point theoretical positioning uncertainty and (ii) the amplitude of high-frequency signal present in the coordinate series (as measured with 3 Hz high-pass filtering). These splines also interpolated short (≤ 10 frames) track bouts where the bird was out of frame. Smoothed spherical coordinates were then converted to Cartesian coordinates (X, Y, Z) without additional smoothing. Similarly, smoothed Cartesian speeds and accelerations (i.e. $\dot{X}$, $\dot{Y}$, $\dot{Z}$ and $\ddot{X}$, $\ddot{Y}$, $\ddot{Z}$) were computed from the first and second derivatives of the spherical coordinate smoothing spline functions (Hedrick et al. 2018). An initial examination of smoothing results showed that high frequency noise was efficiently removed from position series, but remained present in speed and acceleration data, an issue that could partly be improved by increasing the smoothing tolerance by 20%. To ensure that the smoothing tolerance value did not affect our results, we performed a sensitivity analysis, where the base smoothing tolerance was increased by 0% and 40%, with no significant effect on the results presented below (see Table S1; Fig. S7).

Biomechanical variables

A set of biomechanical variables was calculated to describe the flight behaviours of house martins:

Flight speed in the air reference frame (m.s−1):

$$s_a = |\mathbf{v_a}| = |\mathbf{v} - \mathbf{A}| \quad (1)$$

where $\mathbf{v_a}$ is the velocity vector in the air reference frame, computed by subtracting wind speed vector $\mathbf{A}$, calculated from weather station data averaged over the duration of each trajectory, from $\mathbf{v}$, the bird velocity vector ($\dot{X}$, $\dot{Y}$, $\dot{Z}$). The norms of the horizontal and vertical components of $\mathbf{v_a}$, s_{ha} (horizontal speed in the air reference frame) and s_Z (vertical speed) were also calculated. Note that we measured wind speed and direction in the horizontal plane only; hence, $\mathbf{A}$ has no vertical component and s_Z values are equal in the ground and air reference frames.

Mass-specific rate of change in potential energy (W.kg^{-1}):

$$P_p = g s_Z \quad (2)$$

where g is the magnitude of gravitational acceleration.

Mass-specific rate of change in kinetic energy (W.kg^{-1}):

$$P_k = \mathbf{v_a} \bullet \mathbf{a} \quad (3)$$

where $\mathbf{a}$ is the acceleration vector ($\ddot{X}$, $\ddot{Y}$, $\ddot{Z}$).

Mass-specific kinematic power (W.kg^{-1}):

$$P = P_p + P_k \quad (4)$$

Note that power values are mass-specific, as the body masses of individual birds are unknown.

Finally, to measure flight turns in trajectories, we calculated the following variables:

Instantaneous radius of curvature (m):

$$R = \frac{|\mathbf{v}|^3}{\sqrt{|\mathbf{v_a}|^2 |\mathbf{a}|^2 - (\mathbf{v_a} \bullet \mathbf{a})^2}} \quad (5)$$

Note that R is a measure of flight direction change in any plane, not limited to horizontal turns.

Mass-specific centripetal force (m.s^{-2}):

$$F = \frac{|\mathbf{v_a}|^2}{R} \quad (6)$$

Statistical analysis

Most graphical representations and associated statistical analyses were performed in MATLAB r2018b. To visualise the flight envelope of the recorded house martins, several pairs of variables were represented: s_{ha} (horizontal airspeed) vs s_Z (vertical speed), P_{p1s} (rate of change in potential energy) vs P_{k1s} (rate of change in kinetic energy) and s_a (airspeed) vs R (instantaneous radius of curvature). Rates of change in kinetic and potential energy were averaged over 1 s (10 frames) segments because these derivative variables

are more susceptible to noise, even after smoothing. Moreover, they were only averaged over 1 s segments where the flight behaviour (gliding or flapping) did not change to be able to classify each 1 s segment as entirely gliding or flapping. For each pair of variables, the distribution of all data points was visualised by creating a kernel density estimation of the bivariate distribution, by plotting the contours containing 50% and 90% of this estimated distribution, and then by only displaying individual data points if they were outliers, i.e. outside of the 90% contours. For each pair of variables, this process was repeated for flapping data points and gliding data points to separate the two distributions. The univariate distributions of each variable, divided by gliding and flapping, were then statistically compared. The R software v4.1.2 (R Core Team 2021) with the forecast package v8.16 (Hyndman and Khandakar 2008; Hyndman et al. 2022) was used to inspect the autocorrelograms and partial autocorrelograms of the initial time series, which revealed that all variables were temporally autocorrelated, but that keeping one point out of five was enough to remove temporal autocorrelation for all tested variables (P, s_a, s_Z, R) in most trajectories. Autocorrelation was removed independently in each time series (gliding points series and flapping points series) by keeping a minimum interval of 5 frames between each point (except for P_{p1s} and P_{k1s} for which averaging over 1 s already removed autocorrelation). The means of these resulting distributions were then compared using *t*-tests.

To test for the effect of wind on flight speed, data points were divided into three directional bins based on the angle between the bird's instantaneous horizontal direction and the wind vector direction: downwind (0–60 deg), crosswind (60–120 deg) and upwind (120–180 deg). The directional bins were separated between gliding and flapping, totalling to six bins. For each trajectory, a mean airspeed value was calculated for each bin, and statistical comparisons were carried out on the 95 trajectories having at least one point classified into every bin. The distributions of the six bins were visualised using violin plots created with the violinplot function in MATLAB (Bechtold 2016), and the means of each directional bin were compared within each behavioural category using ANOVA. Significant ANOVA were followed by Tukey–Kramer post hoc tests. Furthermore, a linear model was created for each directional bin to analyse the relationship between wind speed (s_w) and bird's airspeed (s_a).

The link between weather variables and vertical speed (s_Z) was studied by dividing data points into flapping or gliding and then by averaging vertical speed over all the data points of both behavioural categories for each trajectory. Three weather variables were also averaged over the entire trajectory: temperature, solar radiation and humidity. Six linear models were then created to analyse the relationship between mean vertical speed and these three weather variables for each behavioural category.

Finally, airspeed (s_a), vertical speed (s_Z) and mass-specific power averaged over 10 consecutive frames where flight behaviour did not change (P_{1s}) were analysed to test if their distributions differed between juveniles and adults. Only the 20 adult individuals recorded during the two field sessions when juveniles were observed were retained to ensure that all individuals were recorded in similar conditions (same weather and same period in the breeding season). For each variable and each behavioural category (gliding or flapping), we pooled data points available for the 5 juveniles (after removing temporal autocorrelation) to obtain a distribution. For adults, we randomly sampled 5 individuals out of 20 adults to obtain a comparable distribution and performed a two-sample Kolmogorov–Smirnov (KS) test (*kstest2* function in Matlab). This KS test was replicated 100 times with different random adult samples. Each KS test returned a D statistic (Sokal and Rohlf 1981), which is considered significant if:

$$D > \sqrt{-\ln\left(\frac{\alpha}{2}\right)\frac{1}{2}\frac{(m+n)}{(mn)}} \tag{7}$$

where m and n are the number of data points for adults and juveniles respectively, and alpha the significance level.

In the present case, as randomly sampled adult birds had variable flight track duration, m varied and D values were not directly comparable between the KS tests. Instead, we derived a sample size–independent C value:

$$C = D/\sqrt{\frac{(m+n)}{(mn)}} \tag{8}$$

We then computed the significance level from the mean C value over the 100 KS tests:

$$\alpha = 2e^{-2C^2} \tag{9}$$

Results

General description of flight behaviour

Figure 2 shows a first investigation of the flight speed distribution of house martins flying near their colony by comparing the distribution of vertical speed and horizontal airspeed for all data points ($N = 45{,}170$; Fig. 2A) or by comparing gliding and flapping flight ($N = 25{,}414$ and 15,810 respectively; Fig. 2B). Note that gliding and flapping totals do not add up to the total number of data points, because flight mode was not visible for 8.7% of video frames. The 90% area for all data points (Fig. 2A) shows that most of the time, house martins have a vertical speed between − 4 and 4 m.

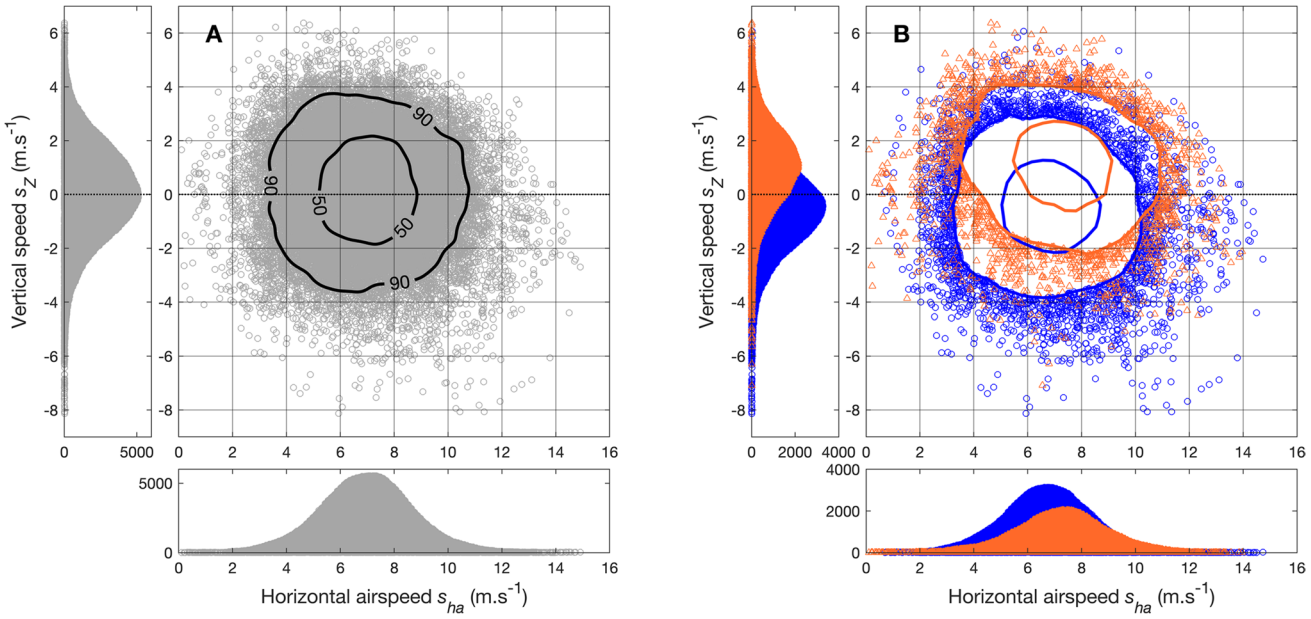

Fig. 2 Distribution of vertical speed (s_Z) versus horizontal speed in the air reference frame (s_{ha}). **A** All data points are represented by grey circles, with two contours indicating the areas containing 50% and 90% of the kernel density distribution. **B** 50% and 90% contours for gliding and flapping; only data points outside of the 90% areas appear. Gliding is represented by blue circles and contours and flapping by red triangles and contours. The univariate distributions of data points are represented along the axes of each panel

s^{-1}, and an horizontal airspeed between 3 and 11 m.s^{-1}. The data points also show the most extreme values exhibited by the recorded house martins, with vertical speeds higher than 6 m.s^{-1} and lower than − 8 m.s^{-1}, and horizontal airspeeds near 15 m.s^{-1}.

Dividing the data points into gliding and flapping flight (Fig. 2B) reveals that both vertical speed and horizontal airspeed are significantly higher when house martins are flapping (mean vertical speed: − 0.36 m.s^{-1} vs 0.85 m.s^{-1}, mean horizontal speed: 6.77 m.s^{-1} vs 7.21 m.s^{-1}, for gliding vs flapping, respectively; see Table 2 for details). It is expected to find that flapping birds have more positive vertical speeds since flapping is often used to gain altitude, but it is worthwhile to note that a significant proportion of data points associated with gliding show a positive vertical speed, as even the 50% area contains points with positive vertical speeds. Positive vertical speeds whilst gliding can be associated with the use of external energy sources (thermal

Table 2 Summary of the quantified variables for gliding vs. flapping flight of house martins. *N* values reflect sample sizes after autocorrelation was removed from time series (see methods)

Variable	Abb	Unit	Gliding flight (mean ± SD)	*N*	Flapping flight (mean ± SD)	*N*	*t*-test
Airspeed	s_a	m.s^{-1}	6.98 ± 1.60	5756	7.42 ± 1.58	3807	$t(9561) = -13.25$ $p < 0.001$
Horizontal airspeed	s_{ha}	m.s^{-1}	6.77 ± 1.62	5756	7.21 ± 1.64	3807	$t(9561) = -12.94$ $p < 0.001$
Vertical speed	s_Z	m.s^{-1}	− 0.36 ± 1.63	5756	0.85 ± 1.45	3807	$t(9561) = -37.22$ $p < 0.001$
Mass-specific rate of change in kinetic energy, averaged over 1 s	P_{k1s}	W.kg^{-1}	1.57 ± 10.73	1821	0.53 ± 10.55	884	$t(2703) = 2.38$ $p = 0.018$
Mass-specific rate of change in potential energy, averaged over 1 s	P_{p1s}	W.kg^{-1}	− 6.00 ± 11.92	1821	10.35 ± 10.84	884	$t(2703) = -34.43$ $p < 0.001$
Radius of curvature, Log-transformed	$\text{Log}_{10}(R)$	-	0.89 ± 0.35	5756	0.99 ± 0.37	3807	$t(9561) = -13.19$ $p < 0.001$
Mass-specific centripetal force	F	g	0.73 ± 0.41	5756	0.68 ± 0.42	3807	$t(9561) = 5.70$ $p < 0.001$

soaring, slope soaring, wind gradients) but also with a decelerating ascent. It is necessary to study the rates of change in kinetic and potential energy to discriminate between these two scenarios.

Figure 3 shows the distribution of rates of change in potential and kinetic energy averaged over 1 s for all data points (Fig. 3A) or by comparing gliding and flapping flight (Fig. 3B), with isolines corresponding to several kinematic power values (i.e. the sum of rates of change in potential and kinetic energy; see Eq. 4). The 90% area for all data points (Fig. 3A) shows that house martins have power values between − 25 and 30 W.kg^{-1} during most of their flight behaviours near the colony.

When comparing gliding and flapping flight (Fig. 3B), the rate of change in potential energy is significantly higher when house martins are flapping (mean − 6.00 vs 10.35 W.kg^{-1}, gliding vs flapping; see Table 2). The difference is less noticeable for the rate of change in kinetic energy,

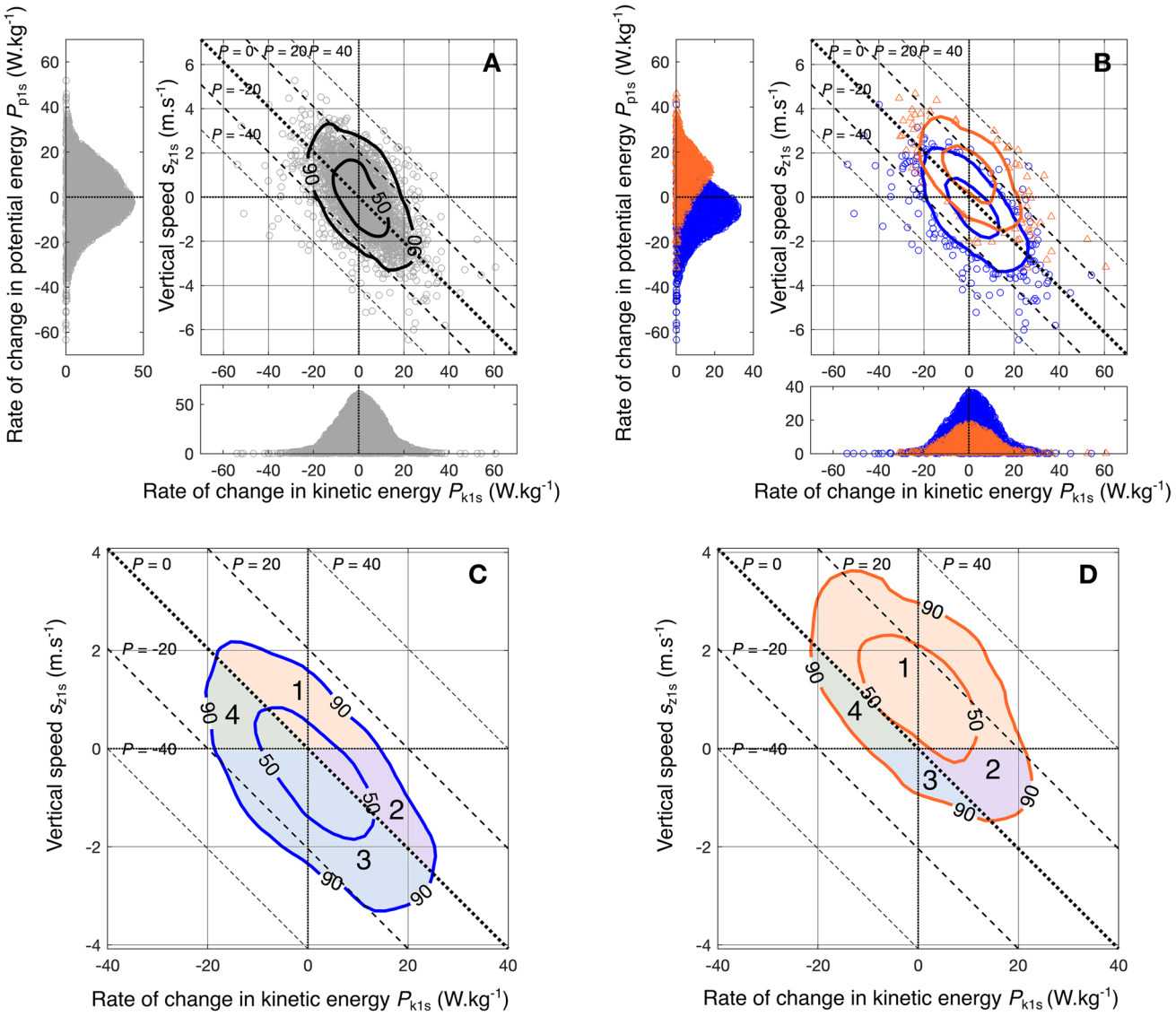

Fig. 3 Distribution of rate of change in potential energy over 1 s (P_{p1s}) versus rate of change in kinetic energy over 1 s (P_{k1s}). **A** All data points are represented by grey circles, with two contours indicating the areas containing 50% and 90% of the kernel density distribution. **B** 50% and 90% contours for gliding and flapping; only data points outside of the 90% areas appear. Gliding is represented by blue circles and contours and flapping by red triangles and contours. Equivalent values of vertical speed averaged over 1 s (s_{Z1s}) are given in the *y* axis. The univariate distributions of data points are represented along the axes of the upper panels. The dashed lines are isolines for power values from − 40 to 40 W.kg^{-1}. The lower panels are magnified views of only the kernel contour of gliding (**C**) or flapping flight (**D**). On these lower panels, zone 1 represents positive power combined with positive vertical speed, zone 2 represents positive power combined with negative vertical speed, zone 3 represents negative power combined with negative vertical speed, and zone 4 represents negative power combined with positive vertical speed. Flight behaviours associated with these zones are discussed in the text

but it is significantly higher for gliding flight (mean 1.57 vs 0.53 W.kg^{-1}, gliding vs flapping). Kinematic power values exhibited by gliding house martins are usually negative (as expected due to adverse air friction and drag), but a significant portion of the gliding distribution shows positive power values, and the $P = 0$ W.kg^{-1} isoline even crosses the 50% area of the distribution. This demonstrates that the use of external energy sources is common for gliding house martins in this context.

The magnified view of the kernel contours for gliding (Fig. 3C) and flapping (Fig. 3D) allows to identify several kinds of flight behaviours. As stated above, gliding flight (Fig. 3C) in the zone above the $P = 0$ W.kg^{-1} isoline is not uncommon and reflects mechanical energy gain, i.e. the use of external energy sources, which can be divided in several categories: data points where P_{p1s} (and consequently vertical speed s_Z) is positive whilst P is also positive correspond to soaring house martins (thermal soaring, slope soaring, zone 1 in Fig. 3C) which can be associated with a decreasing ($P_{k1s} < 0$) or increasing flight speed ($P_{k1s} > 0$). Gliding flight with positive P can also happen for house martins losing altitude ($P_{p1s} < 0$) but accelerating ($P_{k1s} > 0$, zone 2), which could reflect that birds can also use downward or forward wind gusts to accelerate and gain some energy.

At the opposite, gliding flight is often associated with a negative P and a descent ($P_{p1s} < 0$), as expected for typical, passive gliding (zone 3). Note that negative P while gliding can also be observed with positive P_{p1s}, (zone 4) which reflects passive ascents, implying deceleration ($P_{k1s} < 0$) and some expected energy loss ($P < 0$).

Regarding flapping flight (Fig. 3D), it is obviously most of the time associated with positive P, whether it be for ascending (bird accelerates or decelerates, zone 1) or descending flight (bird accelerates, zone 2). However, it is worthwhile to note that a part of the 90% area of the flapping distribution surprisingly shows negative power values. Data points with negative P in ascent (zone 4 in Fig. 3D) could be associated with cases when the bird is struggling to gain altitude and is losing more kinetic energy than the gain in potential energy. Finally, data points with negative P in descent ($P_{p1s} < 0$, zone 3) could be associated with flapping birds encountering an unfavourable downward wind gust that results in mechanical energy loss, despite the flapping muscular work. It is also possible that house martins sometimes flapped their wings to brake (i.e. dissipate energy) and/or to generate lateral forces and perform sharper turns in front of an obstacle (e.g. building wall) or to catch prey.

Finally, as the wind measurement method had several limitations (constant wind speed and direction were assumed during each recording and wind was only measured at a single point in space), we cannot exclude that the speeds and accelerations we measured are slightly different compared to the real airspeeds experienced by the birds if the wind varied in space and time during our recordings. This could influence the positions and spread of individual points in Fig. 3 to some extent.

These results show that house martins perform a wide diversity of flight behaviours near the colony, from fast travelling to slow manoeuvring, and that they regularly use external energy sources. The difference between gliding and flapping flight is not clear-cut with regard to vertical speed and power, and house martins are able to exhibit a wide diversity of behaviours in both flight modes.

Flight turns

Figure 4 helps to understand the turning behaviours of house martins by showing the distribution of airspeed and instantaneous radius of curvature for all data points (Fig. 4A) or by comparing gliding and flapping flight (Fig. 4B), with isolines corresponding to several centripetal force values. The 90% area for all data points (Fig. 4A) shows that house martins have a radius of curvature comprised between 1 and 100 m most of the time, associated with a centripetal force comprised between 0.1 and 2 g. Smaller radius of curvature was usually associated with lower airspeed, which always maintained centripetal forces below 5 g. Exceptionally small radiuses of curvature (near 10^{-1} m in Fig. 4A) show that house martins are occasionally able to perform decimetre-scale turns (mostly u-turns in front of nests), but at very low airspeeds (< 1 m.s^{-1}) and hence low centripetal forces (< 2 g). At the opposite, very large radiuses of curvature (above 100 m) are also uncommon, which suggests that, in this behavioural context, house martins are turning most of the time and rarely fly in straight line.

The most common radiuses of curvature were comprised in the interval 2–20 m (50% area in Fig. 4A), clearly indicating a tortuous flight behaviour. Comparing gliding and flapping turns (Fig. 4B) does not show strong differences in distributions, but flapping is associated with significantly higher airspeeds (mean 6.98 vs 7.42 m.s^{-1}, gliding vs flapping; see Table 2) and larger radiuses of curvature (mean of $\mathrm{Log}_{10}(R)$: 0.89 vs 0.99, gliding vs flapping). Centripetal force was significantly higher in gliding, but the differences were again small (mean 0.73 vs 0.68 g, gliding vs flapping).

Notable behaviours

Figure 3 allows to identify several types of flight behaviours exhibited by house martins, which may be more clearly understood by looking at individual trajectories. Figures S4, S5 and S6 show the 3D views of trajectories, along with several biomechanical variables. Several types of notable flight behaviours can be identified on these trajectories.

Firstly, thermal soaring is visible on some trajectories (e.g. Fig. S4), when a positive power is observed for a

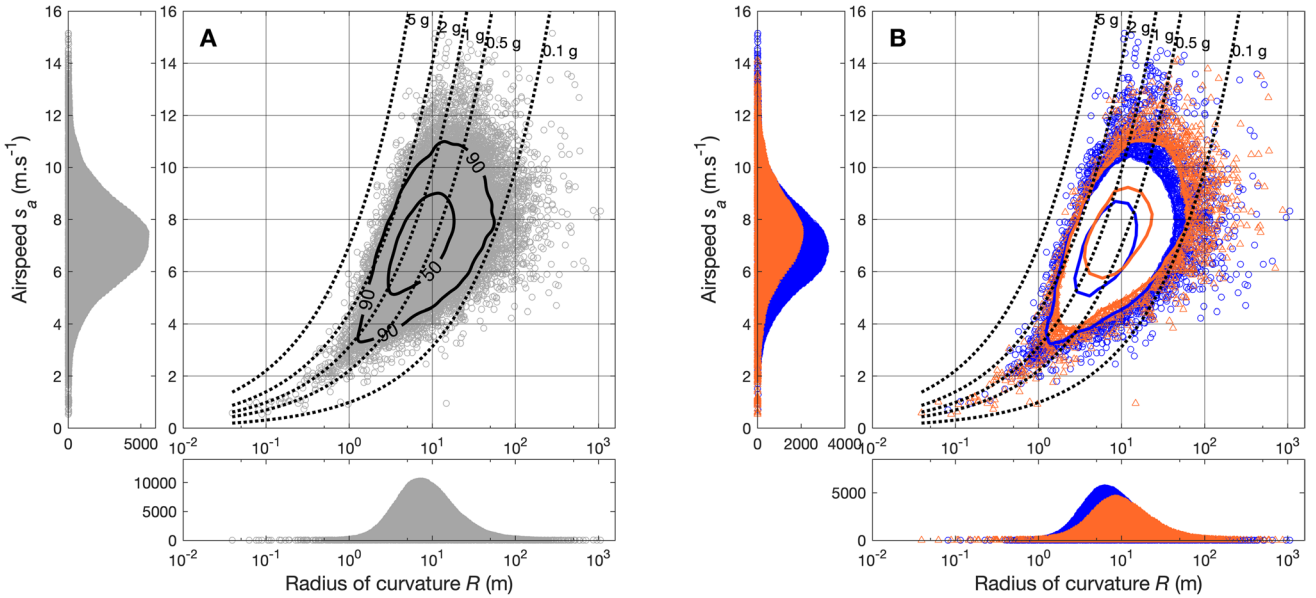

Fig. 4 Distribution of airspeed (s_a) versus instantaneous radius of curvature (R). R is represented in logarithmic scale. **A** All data points are represented by grey circles, with two contours indicating the areas containing 50% and 90% of the kernel density distribution. **B** 50% and 90% contours for gliding and flapping; only data points outside of the 90% areas appear. Gliding is represented by blue circles and contours and flapping by red triangles and contours. The univariate distributions of data points are represented along the axes of each panel. The dotted lines are isolines for centripetal force values from 0.1 to 5 g

gliding bird gaining altitude. Long sequences with birds rising and circling in thermal updrafts, as can be seen for large soaring birds, were rarely observed for house martins. Rather, they seem to frequently extract environmental energy in small bursts whilst they fly near the colony. In addition to thermal soaring, slope soaring was also occasionally observed for birds flying near high buildings where upward wind gusts could occur.

Secondly, a temporal oscillation of vertical speed appeared on several trajectories (e.g. Fig. S5). While the bird is mostly gliding, it is alternatively ascending and descending, again probably using external energy sources since power is often positive. During these sequences, vertical acceleration shows negative values that are regularly close to − 1 g (− 9.81 m.s^{-2}) which is observed for an object in free fall. This suggests that the gliding bird is alternating sequences of ascensions and free falls.

Finally, some atypical flight behaviours described in Fig. 3 can be seen on individual trajectories, such as birds with a positive power during gliding descents (e.g. Fig. S5), which is probably due to downward wind gusts, and birds with a negative power during flapping descents (e.g. Fig. S6), which suggests that flapping is sometimes used to generate adverse forces used for braking or to perform a sharp turn (e.g. for prey capture), or even for a purpose other than transport (e.g. in flight preening).

Effect of wind on flight speed

Figure 5 shows a comparison of the distributions of bird mean airspeed according to the wind direction relative to the bird's direction, for gliding flight (Fig. 5A) and flapping flight (Fig. 5B). Significant differences were only observed for flapping flight, where mean airspeed is significantly higher (ANOVA, $p < 0.001$) for birds flying upwind (7.67 ± 1.01 m.s^{-1}, mean ± SD) compared to birds flying downwind (7.10 ± 0.99 m.s^{-1}) and crosswind (7.32 ± 0.92 m.s^{-1}). However, linear models studying the link between airspeed and wind speed show that wind has a significant effect on both gliding (Fig. 6A–C) and flapping flight (Fig. 6D–F). Birds flying downwind show a significant decrease in airspeed with increasing wind speeds for gliding (Fig. 6A) and a non-significant decrease for flapping (Fig. 6D), whilst birds flying upwind show a significant increase of their airspeed with windspeed for both flight behaviours (Fig. 6C, E). These results suggest that, overall, house martins adjust their flight speed, reducing their airspeed when wind is pushing them, and increasing it when they have to fly against the wind.

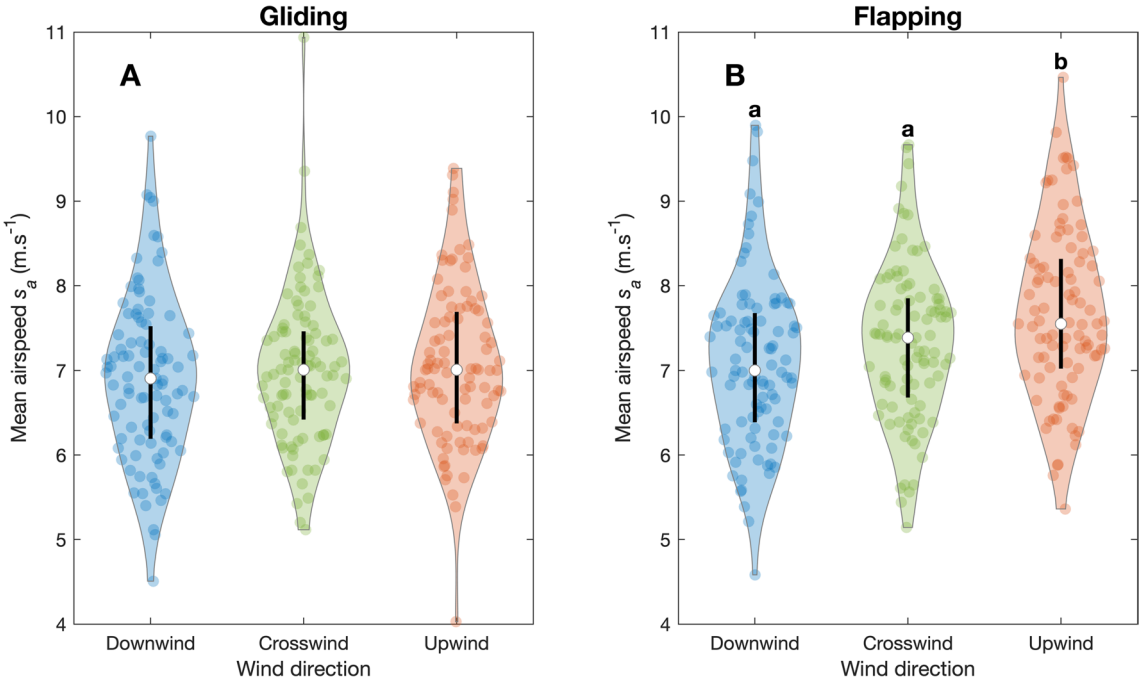

Fig. 5 Distribution of mean airspeed (s_a) versus wind direction category. Each dot represents the mean vertical speed for all downwind/crosswind/upwind flight bouts in a given trajectory. **A** Gliding. **B** Flapping. White dots represent the medians, vertical bars represent the ranges from the 25th to the 75th percentiles, and coloured zones represent the kernel density distributions of each category. Lowercase letters (a and b) indicate significant differences after a significant single-factor ANOVA followed by Tukey–Kramer tests (i.e. groups with label a are significantly different groups with label b). No significant difference was found for gliding. Data for 95 trajectories for which at least one data point was available in each category

Effect of weather on flight behaviours

Studying the effect of several weather variables on vertical speed (Fig. 7) shows that only the vertical speed in gliding flight increases with temperature and solar radiation (Fig. 7A, B) and decreases with humidity (Fig. 7C), whilst there is no significant effect on the vertical speed in flapping flight. Hot and sunny conditions are favourable to the formation of thermal updrafts, and they are associated with less negative or even positive vertical speeds for gliding house martins (note that here each point represents the mean vertical speed for a given trajectory, i.e. is a sum of sequences of thermal/slope soaring and descending gliding flight bouts). This observation is consistent with the use of thermal updrafts by house martins, and this confirms that this behaviour is frequent and important for these birds near their colony since it is still visible at the scale of whole trajectories.

Differences between juveniles and adults

Figure 8 shows the distribution of airspeed (Fig. 8A, C) and vertical speed (Fig. 8B, D) for gliding and flapping flight for the 5 juveniles and the 20 adults recorded during two field sessions (8th and 15th of July). Airspeed during gliding (Fig. 8A) did not differ significantly between adults and juveniles (randomised KS tests, $C = 1.13$, $p = 0.16$), nor did vertical speed during gliding or flapping (Fig. 8B, D; $C = 1.27$, $p = 0.078$ and $C = 1.14$, $p = 0.15$, respectively). Only airspeed during flapping significantly differed between adults and juveniles ($C = 2.23$, $p < 0.0001$), with a flatter, right-shifted distribution for juveniles (Fig. 8C). Median airspeed during flapping was about 0.8 m.s^{-1} higher in juveniles (7.78 vs. 6.94 m.s^{-1}, juveniles vs. adults). No significant difference in kinematic power was found between adults and juveniles ($C = 0.75$, $p = 0.64$ and $C = 0.69$, $p = 0.78$ for P_{1s} during gliding and flapping, respectively).

Discussion

Our study gives a quantitative description of the flight behaviours of the house martin near the colony during the breeding season at fine spatial and temporal scales. Our results show that house martins do use some strategies to save energy during this critical period of their life cycle, such as extraction of environmental energy (Fig. 3), or optimisation of their cost of transport in the ground reference frame (Figs. 5 and 6).

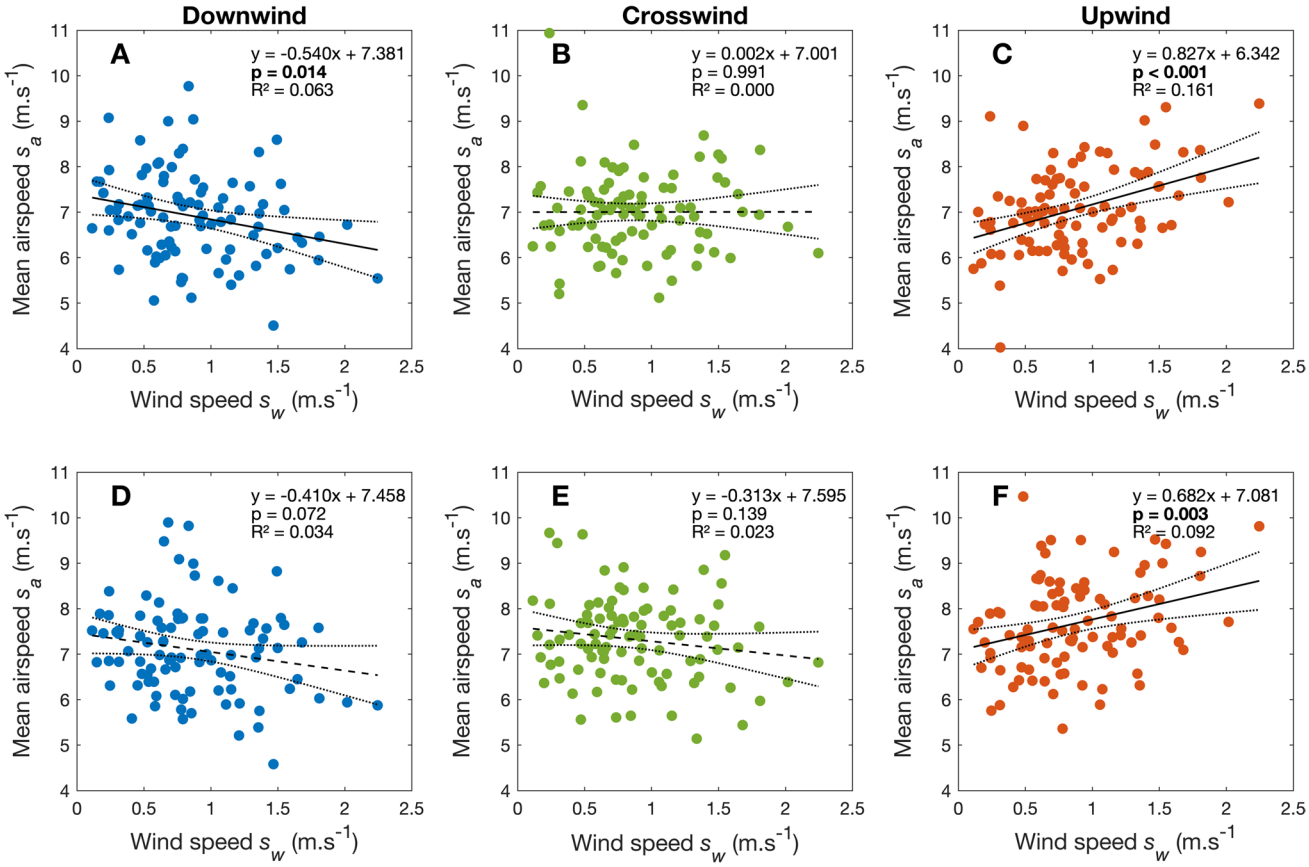

Fig. 6 Mean airspeed (s_a) versus wind speed (s_w) divided by wind direction category (downwind in blue, crosswind in green and upwind in red). **A**–**C** Gliding flight. **D**–**F** Flapping flight. The formula of each linear model, its p-value and R^2 are indicated in each panel. The black dotted lines represent the 95% confidence interval of the slope. Data for 95 trajectories for which at least one data point was available in each category

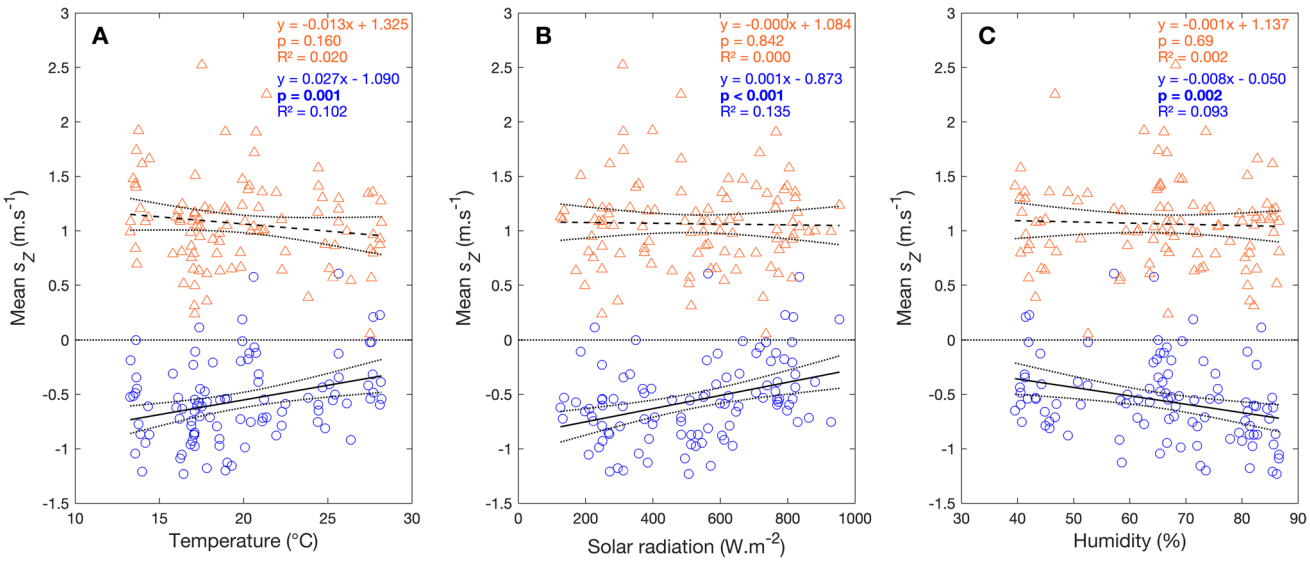

Fig. 7 Mean vertical speed (s_Z) versus temperature (**A**), solar radiation (**B**) and humidity (**C**). Each dot represents the mean vertical speed of all gliding/flapping bouts in a given trajectory. Gliding is represented by blue circles and flapping by red triangles. The formula of each linear model, its p-value and R^2 are indicated in each panel. The black dotted lines represent the 95% confidence interval of the slope

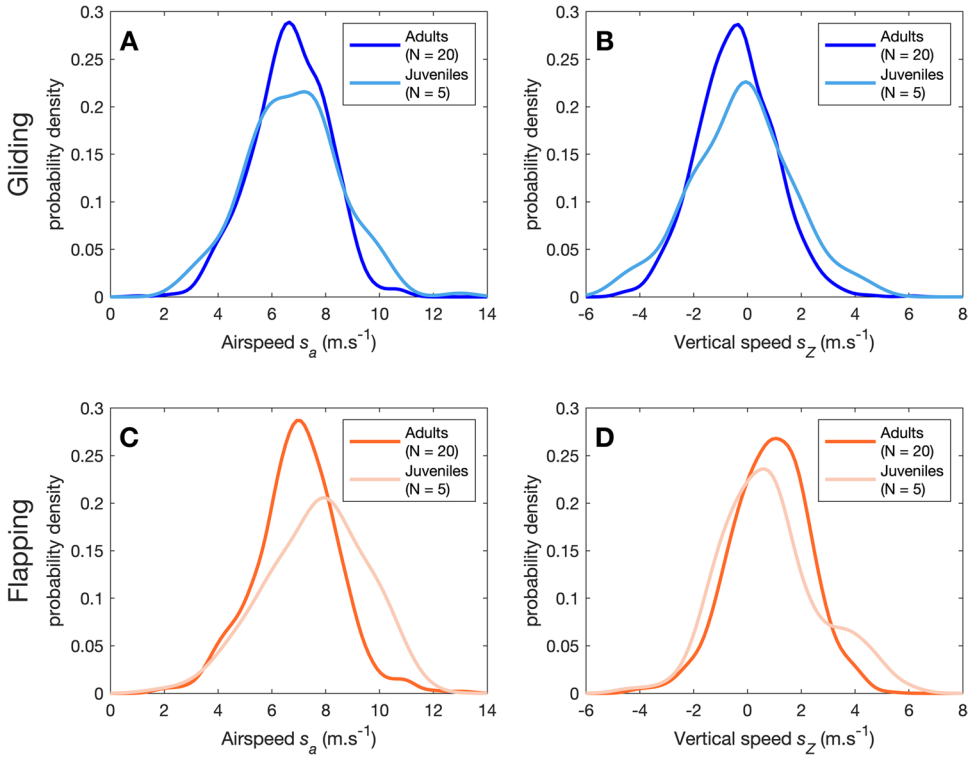

Fig. 8 Distribution of airspeed (s_a) and vertical speed (s_Z) values according to age class for the 25 birds recorded during sessions 7 and 8 (8th and 15th of July). **A**, **B** Gliding. **C**, **D** Flapping

Distribution of biomechanical variables

The 90% area for horizontal and vertical speed (Fig. 2) was rather large (3–11 m.s^{-1} for horizontal speed and − 4 to 4 m.s^{-1} for vertical speed), showing that house martins perform a wide diversity of flight behaviours near the colony, whether it be fast travelling, or slow manoeuvring. The total range of airspeeds (including horizontal and vertical components) was 0.5–15.1 m.s^{-1}. This speed range is quite similar to those observed in other hirundine species, such as foraging barn swallows (3.7–19.4 m.s^{-1}; Warrick et al. 2016) and cliff swallows performing intraspecific chases (2.8–14.0 m.s^{-1}; Shelton et al. 2014).

The distribution of rates of change in kinetic and potential energy (Fig. 3) highlighted the use of external energy sources by house martins (discussed in a later section), but some parts were rather unexpected, such as the positive power values exhibited by some house martins in gliding descent, or the negative power values of some individuals during active flapping. These unexpected behaviours can be associated with specific purposes (e.g. braking in the case of flapping with negative power) but could also be associated with specific environmental conditions (e.g. favourable wind gust in the case of gliding descent with positive power, or adverse wind gust in the case of flapping with negative power). The difference between gliding and flapping flight is not as clear-cut as expected with regard to vertical speed and power, and house martins are able to exhibit a wide diversity of behaviours in both flight modes.

House martins only performed the sharpest turns at low speeds, so their centripetal force never exceeded 5 g (Fig. 4) and was most of the time below 2 g, a value consistent with the average maximum centripetal force of 1.38 g found in foraging common swifts (Hedrick et al. 2018). By contrast, other aerial insectivores perform sharp turns with higher centripetal forces, such as cliff swallows reaching 8 g during intraspecific chases (Shelton et al. 2014), or foraging barn swallows performing 7 g turns (Warrick et al. 2016). These differences are consistent with the contrasting foraging behaviours of house martins and barn swallows, since the former often forage at higher altitudes in more open spaces (del Hoyo et al. 2020), whilst the latter often forage near the ground in relatively cluttered environments (Brown and Brown 2020). In this regard, foraging house martins may be more comparable to common swifts and could thus rely on "gleaning" unsuspecting prey rather than catching evasive prey with sharp turns.

Environmental energy extraction

In our study, positive power values are often observed in gliding house martins (Fig. 3), which shows that they regularly use external energy sources such as thermal updrafts, upward wind gusts and wind gradients. Most of the time,

they apparently only use these energy sources in short bursts, and individuals circling in thermal updrafts for an extended period were rarely observed. Even when a house martin uses a thermal updraft for a longer duration, vertical speed is not constantly positive and often shows temporal oscillations (see Fig. S5) which could be associated either with prey capture or with aerial preening (the latter behaviour was clearly visible on some video recordings). Thermal soaring may be the main source of energy extraction, as shown by the significant effects of temperature, solar radiation and humidity on vertical speed (Fig. 7), but other strategies were occasionally observed such as slope soaring along the high buildings on which the colony was based, or occasional extraction of environmental energy during accelerating gliding descent, presumably from downward wind gusts (Fig. S5).

The use of thermal updrafts was also commonly observed in foraging common swifts (Hedrick et al. 2018), and these updrafts may be an important environmental feature for foraging aerial insectivores, both as a source of mechanical energy and as a substrate for patches of aerial arthropods (de Margerie et al. 2018), because rising air currents can contain a wide diversity of floating prey (Geerts and Miao 2005; Wainwright et al. 2017). For large soaring raptors feeding on the ground, a framework suggested by Shepard et al. (2011) considers that the distribution of mechanical energy sources (thermal updrafts) may be an important constraint in the foraging behaviour of these species. Even if soaring per se is not as vital for aerial insectivores, which can flap their wings at a much lower cost than large raptors (Pennycuick 2008), here thermal updrafts can be considered a source of both types of energy (mechanical energy and food energy), so their spatial and temporal distribution may also have drastic consequences on the foraging behaviour of aerial insectivores. Consequently, atmospheric conditions may strongly impact the availability of resources for aerial insectivores, and rapidly changing conditions could impact their foraging and breeding success.

Effect of wind on flight speed

House martins follow the general tendency to reduce cost of transport, observed in migrating and commuting birds (Wakeling and Hodgson 1992; Hedenström et al. 2002; Kogure et al. 2016; Sinelschikova et al. 2019) and also in foraging swifts (Hedrick et al. 2018), decreasing their airspeed when flying downwind, and increasing it when flying upwind (Figs. 5 and 6). This tendency was visible on gliding flight, and partly on flapping flight, despite a relatively narrow range of wind speed variation during our field sessions (mean wind speed over a trajectory never exceeded 2.5 m. s^{-1}). It is also worth noting that our method of averaging wind speed and direction over a complete trajectory cannot detect more subtle effects of wind variation at finer temporal scales, such as wind gusts. Moreover, we only measured wind speed and direction at one fixed position, which does not take into account wind variations caused by height and the presence of obstacles. Even so, our results suggest that house martins optimise their movements in the ground reference frame, probably because of the presence of their nest at a fixed ground position (central-place foraging; Bryant and Turner 1982).

Differences between adults and juveniles

A significant difference between juveniles and adults was found in the distribution of airspeed during flapping, with juveniles flying at higher, more variable speeds (Fig. 8C). This suggests that the development of flight behaviour in house martins might not be fully mature at fledging (as in many other bird species; Ruaux et al. 2020). Similar differences might exist for other variables (such as a slightly flatter distribution of vertical speed during gliding; Fig. 8B), but the low number of trajectories from clearly identified juvenile birds prevented more precise investigation. The recorded juveniles were likely performing some of their first flights, so they might not be as precise as adults in controlling their flight speed and altitude and would thus need more efforts to adjust their speed and their trajectory. In house martins, post-fledging locomotor ontogeny may consist in a reduction of speed variability (i.e. improvement of flight speed control) in order to converge towards the most energy-efficient speeds in a given context.

As a consequence, juvenile house martins might be less effective aerial foragers than adults, because of a lower energy intake from feeding and/or because of a higher energy output in flight. Indeed, catching arthropods in flight is a complex behaviour, and, for example, it has been shown in juvenile black phoebes (*Sayornis nigricans*) that the proportion of successful foraging attempts increased gradually in juveniles to reach the same level as adults at the age of 7 weeks. This increase is potentially due to trial-and-error learning, but the maturation of cognitive or visual systems cannot be ruled out (Marchetti and Price 1989; Gall et al. 2013). Juvenile house martins return to the nest to roost and are still fed by their parents for a few days after fledging (del Hoyo et al. 2020), which suggests that they are not immediately as efficient as adults in catching prey. During this period, juvenile house martins likely benefit from social learning when foraging near the colony (Varland et al. 1991; Bustamante 1994; Heyes 1994; Kitowski 2009). Further studies comparing the energy intake and energy expenditure of juvenile and adult house martins could clarify these potential differences. It is also possible to hypothesise that some of the differences observed here between juveniles and adults are due to playful behaviours specific to juveniles.

Such behaviours can also represent a way to experiment different flight behaviours and to gain experience.

To conclude, our study gives a first general description of the flight behaviours of house martins near the colony during the breeding season and suggests several mechanisms by which they might save energy. House martins have little margin for lower energy intake and higher energy expenditure during this critical period, so their flight behaviours reflect a set of adaptations to optimise energy gain. Juveniles may not be immediately as efficient as adults in maximising their energy input whilst minimising their output, so parental care and social learning potentially play a critical role during the first few days out of the nest.

Supplementary Information The online version contains supplementary material available at https://doi.org/10.1007/s00265-023-03332-8.

Acknowledgements We would like to thank J. Blasco-Zumeta who helped us to confirm our identifications of juvenile house martins. We thank J. J. Young and S. Windsor (Bristol Univ., UK) who improved our original RSV device design (de Margerie et al. 2015), and designed a second-generation device, upon which the present RSV device is based. We also thank two reviewers that helped to improve this manuscript.

Funding Research on bird flight supervised by EdM was supported by a grant from the *Mission for Transversal and Interdisciplinary Initiatives* at the CNRS in 2018, and an *Emerging scientific challenge* grant from the Rennes University in 2020, which made it possible to acquire some of the material used in this study.

Data availability The flight trajectory and environmental data used as a basis for this analysis are publicly available from the Figshare digital repository: https://doi.org/10.6084/m9.figshare.21118408.v1

Declarations

Ethics approval This is an observational study, without any animal manipulation or disturbance.

Conflict of interest The authors declare no competing interests.

References

Bechtold B (2016) Violin plots for Matlab, Github Project, https://github.com/bastibe/Violinplot-Matlab

Blasco-Zumeta J, Heinze GM (2014) Atlas de Identificación de las Aves de Aragón, http://blascozumeta.com/specie_files/10010_Delichon_urbicum_E.pdf

Brown MB, Brown CR (2020) Barn swallow (*Hirundo rustica*), version 1.0. In: Billerman SM, Keeney BK, Rodewald PG, Schulenberg TS (eds) Birds of the world. Cornell Lab. of Ornithology, Ithaca, NY, USA

Bryant DM (1973) The factors influencing the selection of food by the house martin (*Delichon urbica* (L.)). J Anim Ecol 42:539–564

Bryant DM (1979) Reproductive costs in the house martin (*Delichon urbica*). J Anim Ecol 48:655

Bryant DM, Turner AK (1982) Central place foraging by swallows (Hirundinidae): the question of load size. Anim Behav 30:845–856

Bryant DM, Westerterp KR (1980) The energy budget of the house martin (*Delichon urbica*). Ardea 68:91–102

Bustamante J (1994) Behavior of colonial common kestrels (*Falco tinnunculus*) during the post-fledging dependence period in southwestern Spain. J Raptor Res 28:79–83

de Margerie E, Simonneau M, Caudal JP, Houdelier C, Lumineau S (2015) 3D tracking of animals in the field using rotational stereo videography. J Exp Biol 218:2496–2504

de Margerie E, Pichot C, Benhamou S (2018) Volume-concentrated searching by an aerial insectivore, the common swift, *Apus apus*. Anim Behav 136:159–172

del Hoyo J, Turner A, Kirwan GM, Collar N (2020) Common house-martin (*Delichon urbicum*), version 1.0. In: Billerman SM, Keeney BK, Rodewald PG, Schulenberg TS (eds) Birds of the world. Cornell Lab. of Ornithology, Ithaca, NY, USA

Gall MD, Hough LD, Fernández-Juricic E (2013) Age-related characteristics of foraging habitats and foraging behaviors in the black phoebe (*Sayornis nigricans*). Southwest Nat 58:41–49

Geerts B, Miao Q (2005) Airborne radar observations of the flight behavior of small insects in the atmospheric convective boundary layer. Environ Entomol 34:361–377

Gory G (2008) Le régime alimentaire du martinet noir Apus apus en région méditerranéenne. Rev Ecol-Terre Vie 63:251–260

Hedenström A, Alerstam T, Green M, Gudmundsson G (2002) Adaptive variation of airspeed in relation to wind, altitude and climb rate by migrating birds in the Arctic. Behav Ecol Sociobiol 52:308–317

Hedrick TL (2008) Software techniques for two- and three-dimensional kinematic measurements of biological and biomimetic systems. Bioinspir Biomim 3:034001

Hedrick TL, Pichot C, de Margerie E (2018) Gliding for a free lunch: biomechanics of foraging flight in common swifts (*Apus apus*). J Exp Biol 221:jeb186270

Heyes CM (1994) Social learning in animals: categories and mechanisms. Biol Rev 69:207–231

Hyndman RJ, Athanasopoulos G, Bergmeir C, Caceres G, Chhay L, O'Hara-Wild M, Petropoulos F, Razbash S, Wang E, Yasmeen F (2022) forecast: forecasting functions for time series and linear models. R package version 8.16, https://cran.r-project.org/web/packages/forecast/forecast.pdf

Hyndman RJ, Khandakar Y (2008) Automatic time series forecasting: the forecast package for R. J Stat Soft 27:1–22

Kacelnik A, Houston AI (1984) Some effects of energy costs on foraging strategies. Anim Behav 32:609–614

Kitowski I (2009) Social learning of hunting skills in juvenile marsh harriers *Circus aeruginosus*. J Ethol 27:327–332

Kogure Y, Sato K, Watanuki Y, Wanless S, Daunt F (2016) European shags optimize their flight behavior according to wind conditions. J Exp Biol 219:311–318

Lack D, Owen DF (1955) The food of the swift. J Anim Ecol 24:120

Marchetti K, Price T (1989) Differences in the foraging of juvenile and adult birds: the importance of developmental constraints. Biol Rev 64:51–70

Markman S, Pinshow B, Wright J (2002) The manipulation of food resources reveals sex–specific trade–offs between parental self-feeding and offspring care. Proc R Soc Lond B 269:1931–1938

Pennycuick CJ (1978) Fifteen testable predictions about bird flight. Oikos 30:165–176

Pennycuick CJ (2008) Modelling the flying bird. Academic Press, London

Poessel SA, Brandt J, Miller TA, Katzner TE (2018) Meteorological and environmental variables affect flight behaviour and decision-making of an obligate soaring bird, the California condor *Gymnogyps californianus*. Ibis 160:36–53

R Core Team (2021) R: A Language and Environment for Statistical Computing. R Foundation for Statistical Computing, Vienna, Austria, http://www.R-project.org

Rayner JMV (1982) Avian flight energetics. Annu Rev Physiol 44:109–119

Ruaux G, Lumineau S, de Margerie E (2020) The development of flight behaviours in birds. Proc R Soc B 287:20200668

Shaffer SA, Costa DP, Weimerskirch H (2003) Foraging effort in relation to the constraints of reproduction in free-ranging albatrosses: foraging effort of free-ranging albatrosses. Funct Ecol 17:66–74

Shelton RM, Jackson BE, Hedrick TL (2014) The mechanics and behavior of cliff swallows during tandem flights. J Exp Biol 217:2717–2725

Shepard ELC, Lambertucci SA, Vallmitjana D, Wilson RP (2011) Energy beyond food: foraging theory informs time spent in thermals by a large soaring bird. PLoS One 6:e27375

Sinelschikova A, Griffiths M, Vorotkov M, Bulyuk V, Bolshakov C (2019) Airspeed of the song thrush in relation to the wind during autumnal nocturnal migration. Ornis Fenn 96:64–76

Sokal R, Rohlf FJ (1981) Biometry, 2nd edn. Freeman and Co, New York

Varland DE, Klaas EE, Loughin TM (1991) Development of foraging behavior in the American kestrel. J Rapt Res 25:9–17

Wainwright CE, Stepanian PM, Reynolds DR, Reynolds AM (2017) The movement of small insects in the convective boundary layer: linking patterns to processes. Sci Rep 7:5438

Wakeling JM, Hodgson J (1992) Short communication: optimisation of the flight speed of the little, common and sandwich tern. J Exp Biol 169:261–266

Warrick DR, Hedrick TL, Biewener AA, Crandell KE, Tobalske BW (2016) Foraging at the edge of the world: low-altitude, high-speed manoeuvering in barn swallows. Phil Trans R Soc B 371:20150391

Whittingham LA, Lifjeld JT (1995) High paternal investment in unrelated young: extra-pair paternity and male parental care in house martins. Behav Ecol Sociobiol 37:103–108

Ydenberg RC (1994) The behavioral ecology of provisioning in birds. Écoscience 1:1–14